World Academy of Science, Engineering and Technology
International Journal of Electronics and Communication Engineering
Vol:15, No:2, 2021

Impairments Correction of Six-Port Based Millimeter-Wave Radar

Dan Ohev Zion, Alon Cohen

Abstract—In recent years, the presence of short-range millimeter-wave radar in civil application has increased significantly. Autonomous driving, security, 3D imaging and high data rate communication systems are a few examples. The next challenge is the integration inside small form-factor devices, such as smartphones (e.g. gesture recognition). The main challenge is implementation of a truly low-power, low-complexity high-resolution radar. The most popular approach is the Frequency Modulated Continuous Wave (FMCW) radar, with an analog multiplication front-end. In this paper, we present an approach for adaptive estimation and correction of impairments of such front-end, specifically implemented using the Six-Port Device (SPD) as the multiplier element. The proposed algorithm was simulated and implemented on a 60 GHz radar lab prototype.

Keywords—Radar, millimeter-wave, six-port, FMCW Radar, IQ mismatch.

I. Introduction

A. FMCW Radar

MILLIMETER-wave radar, due to its high bandwidth of signal transmission and extremely low wavelength, has the advantages of:

1) High resolution (range, and also angular, when combined with multiple antenna elements)
2) Ability to observe micro-meter scale movement and vibration of obstacles
3) Ability to perceive different material properties (e.g. dielectric constant)

For radar application with ranges up to ~300 meters, the most common architecture is continuous wave radar. Using FMCW signals (e.g. Chirp signal), the targets' range and velocity information is within $RX(t) \cdot TX(t)^*$, where $TX(t)$ and $RX(t)$ are the complex envelopes of the transmitted and received signals, respectively.

When considering the case of FMCW signal, we can generally write the complex envelope of transmitted signal:

$$TX(t) \quad = \quad e^{j\phi(t)} \tag{1}$$

In the general case of M ideal moving targets, with constant radial velocity, the $RX(t)$ signal is composed of the transmitted signal reflected from targets in field. Each m-th reflection has a set of attenuation (complex phasor d_m), time delay τ_m and Doppler scaling γ_m:

$$RX(t) \quad = \quad \sum_{m=1}^{M} d_m \cdot TX\left(\gamma_m\left(t-\tau_m\right)\right) + n\left(t\right) \tag{2}$$

Dan Ohev Zion* and Alon Cohen of this paper are with Intel Corporation, Israel (*e-mail: dan.ohev.zion@intel.com).

$n\left(t\right)$ is an additive white Gaussian noise. Multiplication of received and transmitted signals yields the function:

$$RX(t) \cdot TX(t)^* \quad = \quad \sum_{m=1}^{M} d_m \cdot e^{j\phi(\gamma_m(t-\tau_m))-j\phi(t)} \tag{3}$$

The range (delay) and velocity (Doppler) of the targets in field can be estimated from this function.

Note that in the case of static targets and transmission of a Chirp signal, we have: $TX(t) = e^{j\left(at^2+bt+c\right)}$, so we get the following term for the multiplication function:

$$RX(t) \cdot TX(t)^* = \sum_{m=1}^{M} d_m \cdot e^{j\left(a\tau_m^2-b\tau_m\right)} \cdot e^{-j2a\tau_m t} \tag{4}$$

which is a sum of M complex tones, where each tone's angular frequency $2a\tau_m$ is linearly related to the range of the corresponding target.

In terms of power consumption and size, it is best to implement the multiplication in an analog manner, in order to avoid down-conversion and sampling of $RX(t)$, which has an extremely large bandwidth (usually several GHz). Typically the bandwidth of the multiplication output ('Base-band signal') is up to only a few MHz. Fig. 1 illustrates a block diagram of a typical FMCW radar of this kind.

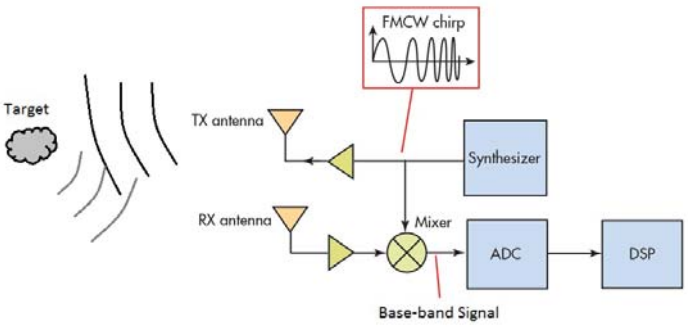

Fig. 1 Block diagram of FMCW radar with analog multiplication

B. Analog Multiplier Impairments

Several challenges arise in analog multiplication, among them:

1) Amplitude and phase mismatch inside the circuit branches lead to IQ mismatch, which degrades image rejection severely
2) Leakage of the $TX(t)$ signal to the $RX(t)$ path, which causes dynamic range limitation in the base-band circuits and Analog to Digital (ADC) converter

3) Non linearity – causes distortion of the output signal: harmonics and intermodulation

The described mechanisms decrease the radar performance, in the following ways:

- Create false targets ("phantoms") in the radar image
- Limit the maximum and minimum range capability
- Limit the overall dynamic range capability of detecting targets simultaneously
- Distort the target dimensions as interpreted by the radar

Note that these impairments are frequency dependent, due to the fact that an extremely large bandwidth is used by the radar. Thus, estimation and correction of these impairments is more complex. These challenges and the problems they cause can be solved in a digital manner (i.e. using algorithms), due to the fact that outputs of the multiplying circuits are being sampled using ADCs. For the case of FMCW (e.g. Chirp signal), the method for estimation and correction of frequency dependent impairments (as described in this paper) becomes much simpler in terms of complexity. This further enables implementation of low-power, low-complexity high performance radar.

There are two architectures for implementation of the analog multiplication unit:

1) Using a direct conversion mixer, known as 'IQ demodulator' ('IQ' stands for 'In-phase' and 'Quadrature'), where $TX(t)$ signal is fed into LO port, and $RX(t)$ signal is fed into RF port of the device (e.g. [1])
2) Using a 'six port detector'

This paper focuses on the second technique, but note that the proposed method can be modified so it can also be used in systems with the first technique.

C. Six-Port Device

The six-port is a passive linear component, first developed in the 1970s for accurate automated measurements of the complex reflection coefficient in microwave network analysis [2]. Later it was integrated in various designs and prototypes of radar sensors (see [3]-[5]).

The major advantages of the six port implementation come in terms of its high available input frequency bandwidth, low power consumption and small circuit size. The six port system has more degrees of freedom in terms of calibration and correction, so its Error Vector Magnitude (EVM) performance can be made better than the IQ demodulator used as a low-IF receiver.

As seen in Fig. 2, the device consists of four hybrid couplers, a single 90 degree phase shifter and four diode detectors. The phase shifter, along with one of the hybrid couplers, can be replaced by a power divider.

In an ideal six-port device, we get the following terms for signals at inputs of the four diode detectors:

$$\begin{aligned} r_1(t) &= RX(t) + jTX(t) \\ r_2(t) &= jRX(t) + TX(t) \\ r_3(t) &= jRX(t) + jTX(t) \\ r_4(t) &= -RX(t) + TX(t) \end{aligned} \quad (5)$$

Based on the fact that "envelope detection" of a band-pass signal is equivalent to extracting the magnitude of its complex envelope (see Appendix): $p_i(t) = |r_i(t)|^2$, $i = 1..4$, so:

$$\begin{aligned} p_1(t) &= |RX(t)|^2 + |TX(t)|^2 + 2Re\{jRX(t)^* \cdot TX(t)\} \\ p_2(t) &= |RX(t)|^2 + |TX(t)|^2 - 2Re\{jRX(t)^* \cdot TX(t)\} \\ p_3(t) &= |RX(t)|^2 + |TX(t)|^2 + 2Re\{RX(t)^* \cdot TX(t)\} \\ p_4(t) &= |RX(t)|^2 + |TX(t)|^2 - 2Re\{RX(t)^* \cdot TX(t)\} \end{aligned} \quad (6)$$

Subtracting pairs of output signals, we get:

$$\begin{aligned} p_3(t) - p_4(t) &= 4Re\{RX(t)^* \cdot TX(t)\} = 4Re\{RX(t) \cdot TX(t)^*\} \\ p_1(t) - p_2(t) &= 4Re\{jRX(t)^* \cdot TX(t)\} = 4Im\{RX(t) \cdot TX(t)^*\} \end{aligned}$$

These are actually the I,Q components of $RX(t) \cdot TX(t)^*$.

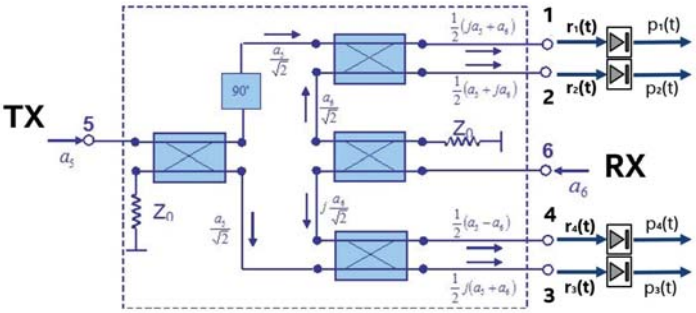

Fig. 2 Schematic of the Six-Port Device

II. System Model

In a practical implementation of a six-port device, there are imperfections due to the implementation of the hybrids (e.g. branches are not of equal magnitude), phase shifter, and the four diodes (mainly mismatch between I-V curves of different diodes). Note that reflections from different components inside the device also contribute to this phenomena. These impairments vary with frequency. The inputs of each of four diode detectors can be modeled as:

$$\begin{aligned} r_1(t) &= h_{a1}(t) \circledast RX(t) + h_{b1}(t) \circledast jTX(t) \\ r_2(t) &= h_{a2}(t) \circledast jRX(t) + h_{b2}(t) \circledast TX(t) \\ r_3(t) &= h_{a3}(t) \circledast jRX(t) + h_{b3}(t) \circledast jTX(t) \\ r_4(t) &= -h_{a4}(t) \circledast RX(t) + h_{b4}(t) \circledast TX(t) \end{aligned} \quad (7)$$

where $h_{a1}(t), h_{b1}(t), ...$ are complex impulse responses of the analog paths of the six-port device (between each inputs to outputs), and $\circledast$ denotes convolution. Note that these impulse responses include the unequal responses of the different diodes.

For the case of Chirp signal, we have a linear time-freq relationship. Therefore, we can think of the $RX(t), TX(t)$ signals as being multiplied by "time varying" impairments:

$$\begin{aligned} r_1(t) &= a_1(t) \cdot RX(t) + b_1(t) \cdot jTX(t) \\ r_2(t) &= a_2(t) \cdot jRX(t) + b_2(t) \cdot TX(t) \\ r_3(t) &= a_3(t) \cdot jRX(t) + b_3(t) \cdot jTX(t) \\ r_4(t) &= -a_4(t) \cdot RX(t) + b_4(t) \cdot TX(t) \end{aligned} \quad (8)$$

So, each time instance of $a_1(t), b_1(t), \ldots$ is actually the impairments set of a specific frequency ('frequency bin'). Let us denote $c_i = a_i^* \cdot b_i,\ i = 1..4$, and use the discrete-time notation:

$$\begin{aligned}
p_1[n] &= |a_1[n]|^2 |RX[n]|^2 + |b_1[n]|^2 |TX[n]|^2 + 2Re\left\{c_1[n] \cdot jRX[n]^* \cdot TX[n]\right\} \\
p_2[n] &= |a_2[n]|^2 |RX[n]|^2 + |b_2[n]|^2 |TX[n]|^2 - 2Re\left\{c_2[n] \cdot jRX[n]^* \cdot TX[n]\right\} \\
p_3[n] &= |a_3[n]|^2 |RX[n]|^2 + |b_3[n]|^2 |TX[n]|^2 + 2Re\left\{c_3[n] \cdot RX[n]^* \cdot TX[n]\right\} \\
p_4[n] &= |a_4[n]|^2 |RX[n]|^2 + |b_4[n]|^2 |TX[n]|^2 - 2Re\left\{c_4[n] \cdot RX[n]^* \cdot TX[n]\right\}
\end{aligned} \tag{9}$$

Note that, $n \in [0, N-1]$, so basically we can treat the continuous Chirp signal as having N uniformly distributed frequencies. The set of samples $\{p_i[n]\}_{n=0}^{N-1}$ is called a "Frame".

Now let us assume that we also have the sampled outputs of the diodes when there is no $RX(t)$ signal present: antennas are directed to free space, where no targets are present. These are denoted as $\{p_{i,no\_rx}[n]\}_{n=0}^{N-1}$, $i = 1..4$ and modeled as:

$$p_{i,no\_rx}[n] = |b_i[n]|^2 |TX[n]|^2,\ \ i = 1..4 \tag{10}$$

Subtracting the "no RX" samples from the actual diode output we get:

$$\tilde{p_i}[n] \equiv p_i[n] - p_{i,no\_rx}[n] \tag{11}$$

Using the complex numbers identity $Re\{z_1 \cdot z_2\} = Re\{z_1\} \cdot Re\{z_2\} - Im\{z_1\} \cdot Im\{z_2\}$, we can rewrite (9), and use a matrix representation, for each n:

$$\begin{bmatrix} \tilde{p_1}[n] \\ \tilde{p_2}[n] \\ \tilde{p_3}[n] \\ \tilde{p_4}[n] \end{bmatrix} = \begin{bmatrix} -Im\{c_1[n]\} & Re\{c_1[n]\} & \frac{|a_1[n]|^2}{2} \\ Im\{c_2[n]\} & -Re\{c_2[n]\} & \frac{|a_2[n]|^2}{2} \\ Re\{c_3[n]\} & Im\{c_3[n]\} & \frac{|a_3[n]|^2}{2} \\ -Re\{c_4[n]\} & -Im\{c_4[n]\} & \frac{|a_4[n]|^2}{2} \end{bmatrix} \cdot \begin{bmatrix} 2Re\{RX[n] \cdot TX[n]^*\} \\ 2Im\{RX[n] \cdot TX[n]^*\} \\ 2|RX[n]|^2 \end{bmatrix} \tag{12}$$

We can use the fact that:

$$|a_i[n]|^2 = \frac{|c_i[n]|^2}{|b_i[n]|^2} = \frac{|c_i[n]|^2}{p_{i,no\_rx}[n]} \cdot |TX[n]|^2,\ \ i = 1..4$$

and rewrite:

$$\begin{bmatrix} \tilde{p_1}[n] \\ \tilde{p_2}[n] \\ \tilde{p_3}[n] \\ \tilde{p_4}[n] \end{bmatrix} = 2A_n \cdot \underbrace{\begin{bmatrix} Re\{RX[n] \cdot TX[n]^*\} \\ Im\{RX[n] \cdot TX[n]^*\} \\ |TX[n]|^2 |RX[n]|^2 \end{bmatrix}}_{x_n} \tag{13}$$

$$A_n = \begin{bmatrix} -Im\{c_1[n]\} & Re\{c_1[n]\} & \frac{|c_1[n]|^2}{2p_{1,no\_rx}[n]} \\ Im\{c_2[n]\} & -Re\{c_2[n]\} & \frac{|c_2[n]|^2}{2p_{2,no\_rx}[n]} \\ Re\{c_3[n]\} & Im\{c_3[n]\} & \frac{|c_3[n]|^2}{2p_{3,no\_rx}[n]} \\ -Re\{c_4[n]\} & -Im\{c_4[n]\} & \frac{|c_4[n]|^2}{2p_{4,no\_rx}[n]} \end{bmatrix}$$

A_n is referred to as the "impairments matrix" of the n-th frequency bin.

III. Method

A. Impairments Estimation

In order to reduce the number of unknown parameters, let us assume that $RX[n] \cdot TX[n]^*$is a zero-mean stationary complex random process. Multiplying each side of (13) with its transpose from right, and applying the expectation operator $E\{\}$:

$$E\left\{ \begin{bmatrix} \tilde{p_1}[n] \\ \tilde{p_2}[n] \\ \tilde{p_3}[n] \\ \tilde{p_4}[n] \end{bmatrix} \cdot \begin{bmatrix} \tilde{p_1}[n] & \tilde{p_2}[n] & \tilde{p_3}[n] & \tilde{p_4}[n] \end{bmatrix} \right\} = 4A_n \cdot E\left\{x_n \cdot x_n^H\right\} \cdot A_n^T \tag{14}$$

It is known that $Re\{RX[n] \cdot TX[n]^*\}$, $Im\{RX[n] \cdot TX[n]^*\}$ are orthogonal and have the same variance, and also orthogonal to $|TX[n]|^2 |RX[n]|^2$, therefore:

$$E\left\{x_n \cdot x_n^H\right\} = \begin{bmatrix} p_n & 0 & 0 \\ 0 & p_n & 0 \\ 0 & 0 & b_n \end{bmatrix} \tag{15}$$

The left side of (14) is the correlation matrix of the four (modified) diode outputs, at the n-th frequency bin. This matrix can be estimated using K 'calibration frames', in which only the n-th sample is focused:

$$\begin{aligned} C_n &\equiv E\left\{ \begin{bmatrix} \tilde{p_1}[n] \\ \tilde{p_2}[n] \\ \tilde{p_3}[n] \\ \tilde{p_4}[n] \end{bmatrix} \cdot \begin{bmatrix} \tilde{p_1}[n] & \tilde{p_2}[n] & \tilde{p_3}[n] & \tilde{p_4}[n] \end{bmatrix} \right\} \\ &\approx \frac{1}{K} \cdot \begin{bmatrix} \sum_{k=1}^K \tilde{p}_{1,cal}^k[n] \cdot \tilde{p}_{1,cal}^k[n] & \cdots & \sum_{k=1}^K \tilde{p}_{1,cal}^k[n] \cdot \tilde{p}_{4,cal}^k[n] \\ \vdots & & \\ \sum_{k=1}^K \tilde{p}_{4,cal}^k[n] \cdot \tilde{p}_{1,cal}^k[n] & \cdots & \sum_{k=1}^K \tilde{p}_{4,cal}^k[n] \cdot \tilde{p}_{4,cal}^k[n] \end{bmatrix} \end{aligned} \tag{16}$$

It is mandatory that these K frames will capture varying values of $RX[n]$. One option is to defining a calibration step, in which a target is moved in front of the radar antenna, so it is captured in many different ranges. The second option is implementing an adaptive mechanism, in which calibration frames are gathered during normal operation of the radar.

Here, we need to solve the equation:

$$C_n - 4A_n \cdot \begin{bmatrix} q_n & 0 & 0 \\ 0 & q_n & 0 \\ 0 & 0 & z_n \end{bmatrix} \cdot A_n^T = 0 \tag{17}$$

This can be solved for A_n, q_n, z_n using numeric methods, using the following initial values, for example:

$$A_{n,0} = \begin{bmatrix} 0 & 1 & \frac{1}{2p_{1,no\_rx}[n]} \\ 0 & -1 & \frac{1}{2p_{2,no\_rx}[n]} \\ 1 & 0 & \frac{1}{2p_{3,no\_rx}[n]} \\ -1 & 0 & \frac{1}{2p_{4,no\_rx}[n]} \end{bmatrix},\ \ q_{n,0} = \frac{1}{K} \cdot \sum_{k=1}^K \tilde{p}_{1,cal}^k[n] \cdot \tilde{p}_{1,cal}^k[n]$$
$$z_{n,0} = 0$$

Note that impairments estimation process does not necessarily need to run at real time, but only when system conditions are changed (e.g. temperature change).

B. Impairments Correction

Let us denote the estimated impairments matrix of the n-th frequency bin as $\hat{A}_n$. Finally, for each frequency bin n, we use $\hat{A}_n$ in (13). The least squares estimator for the I,Q components

of $RX[n] \cdot TX[n]^*$ becomes:

$$\begin{bmatrix} Re\{RX[n] \hat{\cdot} TX[n]^*\} \\ Im\{RX[n] \cdot TX[n]^*\} \\ |TX[n]|^2 \, |RX[n]|^2 \end{bmatrix} = \left(\hat{A_n}^T \hat{A_n}\right)^{-1} \cdot \hat{A_n}^T \cdot \begin{bmatrix} \tilde{p_1}[n] \\ \tilde{p_2}[n] \\ \tilde{p_3}[n] \\ \tilde{p_4}[n] \end{bmatrix} \tag{18}$$

IV. Results

The algorithm was implemented in MATLAB and ran on a PC connected to a lab prototype of a 60 GHz radar (as shown in Fig. 3). The characteristics of the transmission signal are as follows:

- Chirp signal that covers frequency range 57-63 GHz (1200 discrete frequencies in steps of 5 MHz)
- Frame duration: ~2 msec
- Calibration done on 255 frames, during which a target was moved in front of the radar

Fig. 4 shows the IFFT of raw baseband signal, i.e. samples of $RX[n] \cdot TX[n]^*$, where $TX(t)$ and $RX(t)$ are the complex envelopes of the transmitted and received signals from the setup, respectively. The strong signal component in the IFFT is due to the (single) target in front of the radar. On the other hand, the image signal was created due to the impairments of six-port device in the setup. This image can be interpreted as a phantom target, especially when calibrating the delay of long cables.

After applying the proposed algorithm on the raw samples, the image power decreases by more than 25 dB (Fig. 5).

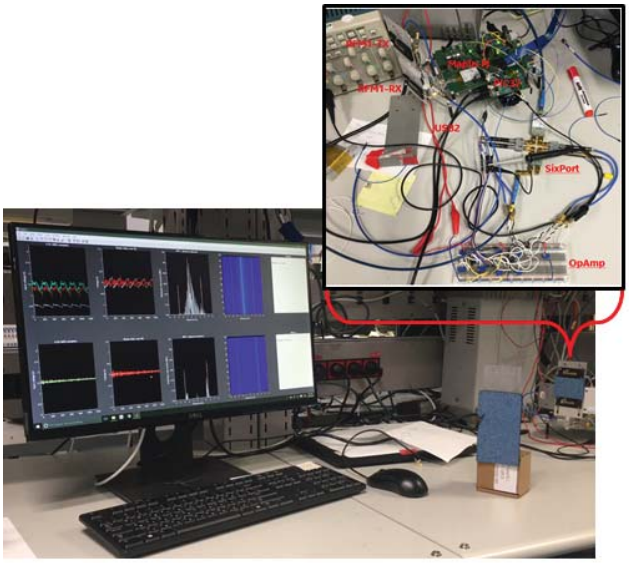

Fig. 3 Picture of 60GHz radar lab prototype, used for testing

V. Conclusions

This paper proposes a method that allows implementation of a high performance Millimeter-Wave radar, that is truly low-power, low-complexity, using the six-port architecture for analog multiplication of received and transmitted signal. Simulation and testing of a lab prototype of 60 GHz radar shows a dynamic range improvement of over 25 dB, when using the invented estimation and correction algorithm. The result is a much cleaner radar image, almost free from false targets.

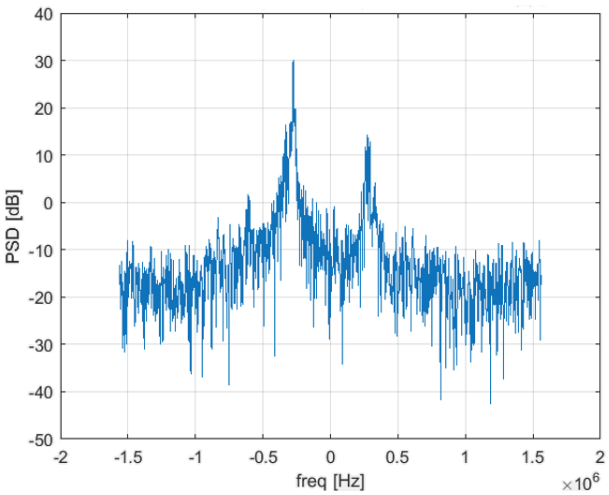

Fig. 4 Spectrum of complex envelope of baseband signal - raw samples from radar setup

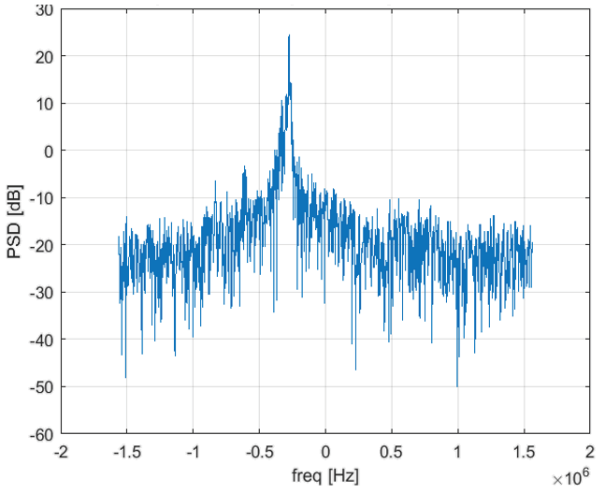

Fig. 5 Spectrum of complex envelope of baseband signal - after correction (using proposed method)

Appendix A
Diode as an Envelope Detector

Operating a diode in its square-law regime, we get the following relationship between its input and output voltage ($x(t)$ and $y(t)$):

$$y(t) = \alpha x^2(t) + \beta x(t) \tag{19}$$

The output of the diode is followed by a base-band low-pass filter, so for the case of RF band-pass signal, the term $\beta x(t)$ vanishes due to its high frequency.

The input band-pass signal can be written as:

$$x(t) = Re\left\{x_c(t) \cdot e^{j\omega_c t}\right\}$$

where $x_c(t)$ is the complex envelope of the signal, and ω_c is a center frequency. Using the complex numbers identity:

$Re^2\{z\} = \frac{1}{2}|z|^2 + \frac{1}{2}Re\{z^2\}$ we rewrite the diode's output:

$$y(t) = \frac{\alpha}{2}|x_c(t)|^2 + \frac{\alpha}{2}Re\left\{x_c^2(t)\cdot e^{j2\omega_c t}\right\} \quad (20)$$

Note that the term $\frac{\alpha}{2}Re\left\{x_c^2(t)\cdot e^{j2\omega_c t}\right\}$is a band-pass signal at frequency $2\omega_c$, so it is filtered by the low-pass filter. Eventually, we get:

$$y(t) \approx \frac{\alpha}{2}|x_c(t)|^2 \quad (21)$$

We conclude that the output of the diode acts as squared magnitude of the complex envelope of the input signal. In other words, it acts as a (squared) envelope detector.

REFERENCES

[1] T. Saito, N. Okubo, Y. Kawasaki, O. Isaji, and H. Suzuki, "An fm-cw radar module with front-end switching heterodyne receiver," in *1992 IEEE MTT-S Microwave Symposium Digest*, June 1992, pp. 713–716 vol.2.

[2] G. F. Engen, "The six-port reflectometer: An alternative network analyzer," *IEEE Transactions on Microwave Theory and Techniques*, vol. 25, no. 12, pp. 1075–1080, Dec 1977.

[3] E. Moldovan, S. O. Tatu, T. Gaman, K. Wu, and R. G. Bosisio, "A new 94-ghz six-port collision-avoidance radar sensor," *IEEE Transactions on Microwave Theory and Techniques*, vol. 52, no. 3, pp. 751–759, March 2004.

[4] A. Stelzer, C. G. Diskus, K. Lubke, and H. W. Thim, "A microwave position sensor with submillimeter accuracy," *IEEE Transactions on Microwave Theory and Techniques*, vol. 47, no. 12, pp. 2621–2624, Dec 1999.

[5] A. Koelpin, G. Vinci, F. Barbon, S. Lindner, G. Fischer, and R. Weigel, "The six-port technology: A low-cost concept for precise position measurements," in *International Multi-Conference on Systems, Sygnals Devices*, March 2012, pp. 1–5.